Stony Brook University

Crystal Structure Prediction of Compounds in the Al-O System: AlO_2 and Al_4O_7

A Thesis Presented

by

Yue Liu

to

The Graduate School

in Stony Brook University

for the Degree of

Master of Science

in

Geosciences

Stony Brook University

December 2013

Stony Brook University

The Graduate School

Yue Liu

We, the thesis committee for the above candidate for the

Master of Science degree, hereby recommend acceptance of this thesis.

Artem R. Oganov – Thesis Advisor
Professor, Department of Geosciences

Brian Phillips –Chairperson of Defense
Professor, Department of Geosciences

John Parise
Professor, Department of Geosciences

This thesis is accepted by the Graduate School

Charles Taber
Dean of the Graduate School

Abstract of the Thesis

Crystal Structure Prediction of Compounds in Al-O System: AlO_2 and Al_4O_7

by

Yue Liu

Master of Science

in

Geosciences

Stony Brook University

2013

USPEX is the foremost Evolutionary Algorithm which calculates crystal structure through genetic algorithm. And it is using *ab initio* determination to contribute powerful searching in crystal structure prediction. This method enables crystal structure prediction at arbitrary P-T conditions, given just the chemical composition of the material. USPEX is interfaced with DFT or classic codes, such as VASP, SIESTA, GULP and so on. USPEX can also be used to search for materials with desired physical properties. There are already significant discoveries found by using USPEX. For instance, it has been found the 40-atom cell of $MgSiO_3$ post-perovskite for this fixed composition system. And for variable composition, like Mg-O system, the previous work showed that new oxides MgO_2 and Mg_3O_2 could become stable at high pressure.

In the crust, oxygen and aluminum have the first and third highest abundance among all elements, respectively. Also aluminum is the most abundant metal element, which takes 7.57% of the total mass of crust. Until now, there are more than 270 kinds of minerals were found containing aluminum. Aluminum is a good conductor of electricity and heat, while alumina is an insulator. But alumina is suitable for abrasive materials and cutting tools. Activated alumina could also be used as catalysts, adsorbents, dehydrating agent and a catalyst carrier. Accordingly, Al-O system is important and prospective for scientists to explore for further oxides and their properties.

Materials under pressure often exhibit exotic physical and chemical behaviors. In particular, extremely new stable compounds could appear. For Al-O system, we use the variable composition searching by USPEX and have found two extraordinary compounds Al_4O_7 and AlO_2

are thermodynamically stable. Al_4O_7 is stable under the pressures between 330-443 GPa and AlO_2 becomes stable from 322 GPa. Detailed chemical bonding analysis shows Al_4O_7 has one peroxide ion $[O–O]^{2–}$ in each lattice. And in AlO_2, there are two peroxide bonds with different directions per lattice. As a result, under high pressure, the new state of aluminum oxides is generated with both oxygen and peroxide ions. And these two new Al-O compounds become stable because the formation of peroxide anions $[O–O]^{2-}$.

Our calculations of structure optimization and phonon spectrum also indicate the AlO_2 and Al_4O_7 are stable under certain pressure. The band structures of these two aluminum oxides suggest they are both insulators. According the calculation of density of states, as we expected, most valence electrons are on oxygen atoms and rather than on Al. Also oxide and peroxide ions have different effects on the generation of conduction band.

Table of Contents

List of Tables

List of Figures

Chapter 1

Calculation Methods Introduction

Novel materials design and discovery is everlasting subject in materials research. Recently, computer simulation has gradually become the main research method besides theoretical and experimental studies, due to the great development of fundamental theories and computers. It could not only provide explanations but also give directions for experiments and accordingly decrease the expense on blind experiments. In addition, computer simulation could explore the unknown areas by simulating the extreme conditions which experiments are unaffordable. Computational material science has developed into a cross subject based on condensed matter physics, quantum chemistry, material sciences, electronic structure calculation and computer science [1]. To design novel functional materials with various properties according to the needs of practical application has become real from just a dream.

1.1 Materials Design

Materials design means to predict composition, structure and properties of new materials through theories and computational calculation. In short, its purpose is to design new materials with specific properties. It is a cross-disciplinary subject which has a rapid development recently. It is related to condensed matter physics, theoretical chemistry, materials science, engineering mechanics and computer algorithms, and other related disciplines.

From a broad view, the material design can be divided into three levels depends on the spatial scale of research object [2]. First, the micro-level design is around 1nm of magnitude. And it is also an atomic and electronic level. Second is the continuous model level and its magnitude is

1μm. This kind of materials can be treated as continuum, and don't need to consider for how individual atom or molecule would act. Then the last level is engineering design. The scale corresponds to macroscopic materials, and the design of material processing and performances of bulk materials.

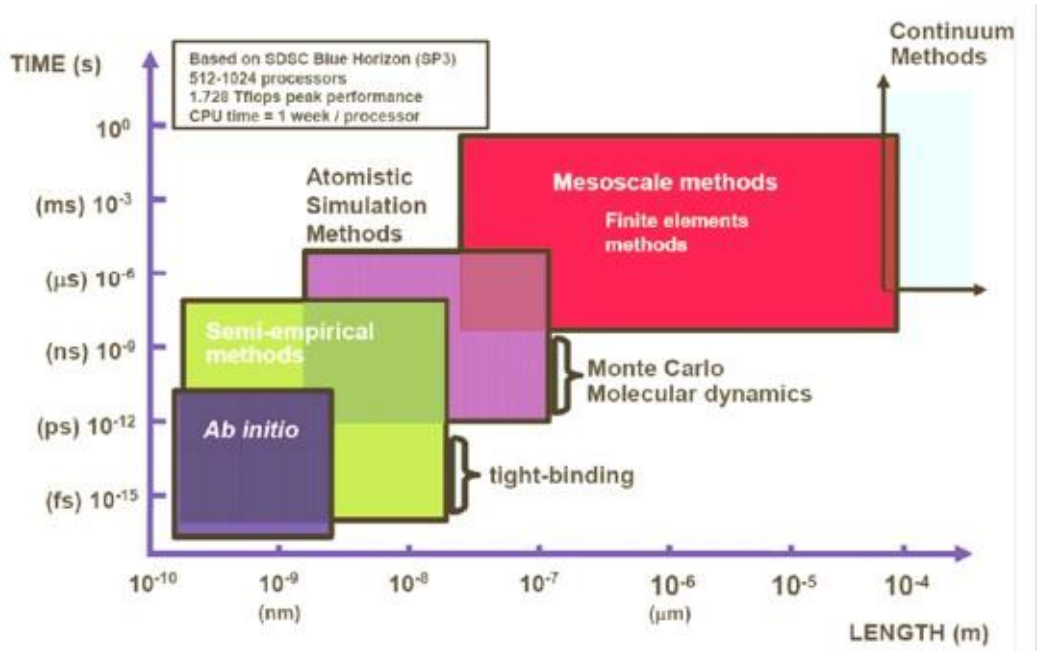

Figure 1. 1: Spatial and time scales of materials design and the calculation methods [3]

The spatial scales and timescales of several levels we discuss above and their corresponding theoretical methods are shown in Figure 1.1. The output result from the previous level in spatial scale can be calculated as the input of next level. Also there are different methods for different levels. From atomic-scale to nano-scale, the first-principles method (*ab initio* method), a number of semi-empirical methods and atomistic simulation methods could be applied. From nano-scale to mesoscopic, there are finite element method, molecular dynamics, defect dynamics, and Monte Carlo simulation to calculate. And for scales from mesoscopic to macroscopic, FEM and Continuum theory are more suitable. Sometimes, the applicable methods for different scales could overlap.

My thesis is mainly related to the microscopic realm of solid quantum mechanics. We will focus on the calculation method based on the first-principles calculations. First-principles calculation only needs to input the atomic number, atomic positions and some basic physical constants. It is a conclusion from mandatory rules or from deduction, compared with experimental parameters which are a large number of orderly data. These data can be derived from the first principles (also called theoretical statistics) and can also be derived from experiments (also called experimental statistics). However, for some certain problem, first-principles and empirical parameters don't have obvious boundary, so the boundary must be specifically defined: If some principles or data are derived from first-principles, but during the deduction process there are some assumptions are added (these assumptions must be persuasive), then these principles or data is called "semi-empirical." Here we will focus on several first-principles calculations, includes Hartree-Fock method, Density functional theory (DFT), GW method [4], etc.

1.2 Hartree-Fock Method: *ab initio* Calculations

Currently, most physicists consider the concepts of first-principles calculations and *ab initio* calculations are similar to each other. But the theoretical chemists may not agree because in the history of quantum chemistry, "*ab initio*" has a specific meaning, and also known as the Hartree-Fock method [5]. Hartree-Fock method is an approach based on three basic assumptions to solve the electronic Schrödinger equation. These three approximations are as follow: 1) non-relativistic approximation, which is considered the electron mass equals to its static mass, namely m_e (electron mass) = $m_{e.0}$ (static mass). And the speed of light approaches infinity that is to solve the non-relativistic Schrödinger equation rather than relativistic Dirac equation. 2) Born-Oppenheimer approximation, which separately processes the nuclear movement and electrons

movement. Since the mass of nucleus is generally about 10^3 to 10^5 times larger than the mass of electron, the movement of nucleus nearly a thousand times slower than the movement of electron in molecules. Therefore, to study electron movement, nucleus can be approximately considered as still. The Schrödinger equation of this certain system can be decomposed into the equation of describing electron motions and the equation of describing the nuclear motion states. 3) Orbital approximation (also known as single-electron approximation), that is to treat the movement of electrons in system as it is effected by the average potential field of other electrons. Thereby simplify the multi-particle Schrödinger equation into the form the single-electron equation and the total wavefunction is a Slater determinant formed by one-electron orbitals.

Hartree-Fock method is based on the three basic approximations above to solve the Schrödinger equation. It firstly treated the wave function of a single determinant function, which is formed by molecular orbitals, as the system. According to the total energy, we can get the single-particle functions from variation of the orbitals which is called Hartree-Fock equation. This Hartree-Fock equation is still a complex partial differential equation that is quite difficult to solve. Usually, we need to use the basic functions to expend this equation, and the most commonly used basic functions are Slater or Gaussian function. When basis set is large enough, the solution of expanded equation is approximated to the Hartree-Fock equation. In applications, however, the accuracy of Hartree-Fock method may not be high enough, so various corrections are necessary, such as the relativistic effect correction, nuclear and electronic motion coupling correction and correction of electron motions correlation.

1.3 Density Functional Theory

The basis of density functional theory is that all ground-state properties are functions of the electron density in system. This theory came from a famous article in 1964 written by P. Hohenberg and W. Kohn [6]. After decades of development, the first-principles which based on density functional theory has become the most popular method in physics, chemistry and materials sciences, and has been widely used in systems like atomic, molecular, nano-structures (including clusters, surfaces and interfaces) and strongly correlated electrons. It has developed into a complete branch and continues to develop. W. Kohn has also been awarded the 1998 Nobel Prize in Chemistry because of his contributions. In this section, I will briefly introduce and review of the basic theory from a beginner's perspective.

1.3.1 Hohenberg-Kohn theorem

After adiabatic approximation, in the multi-particle system of non-relativistic form, the kinetic energy of the nucleus of Schrödinger equation becomes zero and the potential function of interaction between nucleus turns into a constant. So now what need to be solved is the Schrödinger equation which contains only electron kinetic energy, the potential of electrons in nucleus and the electron - electron interaction potential. And its Hamiltonian could be written as:

$$H=-\frac{h^2}{2m_e}\sum_i \nabla_i^2+\sum_i V_{ext}(r_i)+\frac{1}{2}\sum_{i\neq j}\frac{e^2}{|r_i-r_j|} \tag{1.1}$$

Although equation (1.1) has been simplified, it is still very difficult to be solved exactly. The key is the electron - electron interaction term (the third term of formula 1.1) which is a two-particle operator. There are many methods that can be used to further simplify this equation. One of the

most important methods is Hartree-Fock (HF) method, because it can accurately describe the atoms and molecules, and this method is widely used in quantum chemistry.

For the study of the periodic system, density functional theory is more efficient. This theory is established on the basis of two fundamental theorems [8] that are proved by Hohenberg and Kohn.

Theorem I: external potential $V_{ext}(r_i)$ can be determined by the ground state electron density *ρ(r)* plus an irrelevant constant.

Inference I: It can be seen from equation (1.1), when $V_{ext}(r_i)$ is determined, in addition to a constant, the Hamiltonian of the system is completely determined. So are all states wave function (including the ground state and excited state). It can also be expressed as: all properties of the system are uniquely determined by the electron density functional *ρ(r)* of ground state, which can be writing as below (1.2):

$$E[\rho] = \langle \psi | T + V | \psi \rangle + \langle \psi | V_{ext} | \psi \rangle = \langle \psi | T + V | \psi \rangle + \int \rho(r) V_{ext}(r) dr \tag{1.2}$$

The first term in the above equation is a density functional which is independent from an external field.

Theorem II: When the total number of electrons is constant, the ground state energy of the system is the minimum energy functional of charge density *ρ(r)*, and the corresponding charge density *ρ(r)* is the ground state charge density of this system.

Inference II: When the number of particles is constant, we can get the energy $E_G[\rho]$ of ground state of the system through the energy functional variation of the density function *ρ(r). And the ρ(r)* is the charge density of ground state.

Based on the formula (1.2), which equals to Theorem I, the multi-electron system energy functional can be rewritten into the formula below (1.3):

$$E[\rho]=T[\rho]+\frac{1}{2}\iint drdr'\frac{\rho(r)\rho(r')}{|r-r'|}+E_{xc}[\rho]+\int\rho(r)V_{ext}(r)dr \tag{1.3}$$

In formula (1.3), the first term is the kinetic energy, and the second term is the Coulomb interaction between the particles. The third one $E_{xc}[\rho]$ represents all the interactions that are not included in the previous two terms, also this reflects the complexity of interactions. Also, the third term represents the quantum effects of the particle-particle interaction, which mainly consists exchange and correlation interaction. They are both the functionals of density *ρ(r)*, but are still unknown.

1.3.2 Kohn-Sham equation

According to Hohenberg-Kohn theorem, we can write the following variational equation:

$$\int dr\delta\rho(r)\left[\frac{\delta T[\rho(r)]}{\delta\rho(r)}+v(r)+\int dr'\frac{\rho(r')}{|r-r'|}+\frac{\delta E_{xc}[\rho(r)]}{\delta\rho(r)}\right]=0 \tag{1.4}$$

Then add the prerequisite $\int dr\delta\rho(r)=0$, we can get Euler-Lagrange equation as following:

$$\mu=\frac{\delta T[\rho(r)]}{\delta\rho(r)}+V_{ext}(r)+\int dr'\frac{\rho(r')}{|r-r'|}+\frac{\delta E_{xc}[\rho(r)]}{\delta\rho(r)} \tag{1.5}$$

Lagrange multiplier μ is a chemical potential. So, in fact, (1.5) defines a formula of a particle in an effective potential field. And the effective potential could simply be defined as:

$$V_{eff}(r)=V_{ext}(r)+\int dr'\frac{\rho(r')}{|r-r'|}+\frac{\delta E_{xc}[\rho(r)]}{\delta\rho(r)} \tag{1.6}$$

Accordingly, you can turn the problem of a multi-particle Schrödinger equation into solving the Euler-Lagrange equations, which only relevant to charge density *ρ(r)*. But in the actual calculations, we still do not know the kinetic energy term *T[ρ(r)]* To solve this problem, in 1965, Kohn and Sham proposed an assumption: sthe kinetic energy functional *T[ρ(r)]* can be described by a known functional *Ts[ρ(r)]* of non-interacting particles. It also has the same density function with the interaction system, and attributes the part that cannot be converted between *T[ρ(r)]* and $T_s[\rho(r)]$ into the complex items $E_{xc}[\rho]$. In addition, with wave function $\phi_i(r)$ of N particles, scientists construct the single-particle density function to draw the single-particle image [7]:

$$\rho(r)=\sum_{i=1}^{N}\left|\phi_i(r)\right|^2 \tag{1.7}$$

Then we can obtain the specific form of kinetic energy functional:

$$T_s[\rho]=\sum_{i=1}^{N}\int dr\phi_i^*(r)\left(-\nabla^2\right)\phi_i(r) \tag{1.8}$$

Now, the variation for ρ can be instead by the variational for $\phi_i(r)$, and E_i replaces the Lagrange multiplier, so there is:

$$\delta\left\{E\left[\rho(r)\right]-\sum_{i=1}^{N}E_i\left[\int dr\phi_i^*(r)\phi_i-1\right]\right\}\Big/\delta\phi_i(r)=0 \tag{1.9}$$

Thus, we can get the result:

$$\left\{-\nabla^2+V_{KS}\left[\rho(r)\right]\right\}\phi_i(r)=E_i\phi_i(r) \tag{1.10}$$

And

$$H_{KS} = T_0 + V_H + V_{xc} + V_{ext} = -\nabla_i^2 + \int dr' \frac{\rho(r')}{|r-r'|} + \frac{\delta E_{xc}[\rho(r)]}{\delta\rho(r)} + V_{ext}(r) \tag{1.13}$$

And

$$V_{KS}[\rho(r)] \equiv V_{ext}(r) + \int dr' \frac{\rho(r')}{|r-r'|} + \frac{\delta E_{xc}[\rho(r)]}{\delta\rho(r)} \tag{1.11}$$

And (1.10) can also be written as:

$$H_{KS}\phi_i(r) = E_i\phi_i(r) \tag{1.12}$$

In this way, we can get the single-particle wave function $\phi_i(r)$ which is similar to Hartree-Fock equation. The combination of equations (1.7), (1.10) and (1.13) are called Kohn-Sham equations. We can solve equation (1.10) to get $\phi_i(r)$, and then construct the density function of ground state according to formula (1.7). From Hohenberg-Kohn theorems, density function of particle numbers precisely determines the energy of ground state of system, wave function and so on.

From equation (1.13), the Hartree potential, exchange-correlation potential and external potential V_{ext} are all density functionals. And density is also dependent on $\phi_i(r)$ from the Kohn-Sham equation. On the other hand, the establishment of Kohn-Sham equations relies on V_H, V_{xc} and V_{ext}, which is a self-consistent process. Usually, we need to firstly presume a density function $\rho_0(r)$ to construct H_{KS1}, and then solve the eigenvalue problem in order to get a series of wave functions $\phi_i(r)$ and form a new density function $\rho_1(r)$. Under normal circumstances, $\rho_0(r)$ and $\rho_1(r)$ have some differences. This can construct a new H_{KS2} from $\rho_1(r)$, and then form $\rho_2(r)$. Repeating this process, density function will converge to $\rho_f(r)$. The H_{KSf} constructed by $\rho_f(r)$ could also generate density function $\rho_f(r)$. At this point, we can believe that $\rho_f(r)$ is the

density function of ground state of system. The physical expectations obtained from intrinsic wave function of H_{KSf} are the physical properties of ground state in system.

1.3.3 Exchange - correlation interaction functional

1) LDA and GGA

Exchange - correlation interaction functional includes all the complexities of many-body interactions, but the specific format is still unknown. Kohn and Shem have proposed the Local Density Approximation (LDA), also called Local Spin Density Approximation (LSDA) in a broad way. Under this kind of approximation, at each point in space, the integrations of exchange - correlation energy density of the homogeneous electron gas with same density is exchange - correlation energy.

$$E_{xc}^{LSDA} = \int d^3 r n(r) \varepsilon_{xc}^{\hom}\left(n^{\uparrow}(r), n^{\downarrow}(r)\right). \qquad (1.14)$$

$n^{\uparrow}(r)$ and $n^{\downarrow}(r)$ respectively represent for spin up and spin down electrons density, but in a non-spin system, it can be simply defined as: $n^{\uparrow}(r) = n^{\downarrow}(r) = n(r)/2$

The widely used method is through the homogeneous electron gas which is obtained by fitting Monte-Carlo method and the parameterization of PZ functional which is calculated by Perdew and Zunger [8].

Exchange energy: $\varepsilon_x(r_s) = -0.9164 / r_s$

Correlation energy: $\varepsilon_c(r_s) = \begin{cases} -0.2846/\left(1+1.0529\sqrt{r_s}+0.3334 r_s\right) & (r_s \geq 1) \\ -0.0960 + 0.0622 \ln r_s - 0.0232 r_s + 0.0040 r_s \ln r_s & (r_s \leq 1) \end{cases}$

And r_s is the Weigner-Seitz radius. In the three-dimensional homogeneous electron gas model, it could be written as:

$$r_s = \left(\frac{3}{4\pi\rho} \right)^{\frac{1}{3}} = 1.919 / k_F, \;\; k_F - \left(3\pi^2 \rho \right)^{\frac{1}{3}} \tag{1.15}$$

For the core electron, r_s is usually less than 1, and for valence electron, it is normally between 1 and 6.

Although L(S)DA was a great success, but there are still some shortcomings, such as the exchange energy has been underestimated for about 10% and the correlation energy is overestimated by 2 to 3 times. Under normal circumstances, the exchange energy should be about 10 times bigger than correlation energy, so exchange-correlation energy under local density approximation is still underestimated. Based on L(S)DA, there is a development of the generalized gradient approximation (GGA). After GGA approximation, the exchange-correlation energy is the functional of electrons density and its gradient. Currently, the most widely used GGA functionals are PW91 [9] and PBE [10].

2) Hybrid functional

Hybrid functional is dependent on the combination of Hartree-Fock functional and other functionals (such as LDA or GGA). This is the most accurate functional until now. As in the famous quantum chemistry software Gaussian, B3LYP functional is widely used.

1.3.4 Pseudopotential

Since the smoothing function can be more easily expanded into a plane wave, replacing the Coulomb interaction of electrons between the nucleus and inner core with an effective ionization

potential. This can greatly reduce a plane wave basis set size and the complexity of calculation. Core electron atoms hardly participate in bonding, and properties of molecules and solids are mainly decided by the valence electrons, so the pseudopotential obtained from the atomic calculation can be used in calculation of other molecules or solids. The theoretical information about pseudopotential can be found in the reference [1]. The empirical pseudopotential can be obtained from fitting the experimental data, and there are two basic models are the "empty core" model [11] and square-well model [12]. Empirical pseudopotential used to play an important role in the history of electronic structure calculations. Through fitting calculation, pseudopotentials are generated from the atomic properties. These pseudopotetials are belonging to "*ab initio*" category. We are going to introduce several types of "*ab initio*" pseudopotentials which have great impacts on the accurate calculation of modern electronic structure.

1) norm-conserving pseudopotential

In general, the pseudo-potential is smoother than real potential, so it's better to use the plane wave as basis function. During electronic structure calculation, when seeking electronic density of states resulting from wave function, it needs the effective single-electron potential. This single-electron potential should be consistent with real potential in housing area ($r > r_c$). To define norm-conserving pseudopotential, there are several norm-conserving conditions to comply [13]:

a. The eigenvalues of valence electron with pseudopotential method should be the same with all-electron method.

b. Pseudopotential and all-electron potential should be consistent outside of a cutoff radius.

c. The logarithmic derivative of wave function of pseudopotential and all-electron potential should be equal outside of a cutoff radius.

d. The charge density integration of pseudopotential and all-electron potential must equal to each other. This is the most fundamental rule, and also known as norm-conservation condition, namely (1.17)

$$\int_{r<r_c} dr \left|\phi_{ps}(r)\right|^2 = \int_{r<r_c} dr \left|\phi_t(r)\right|^2 \tag{1.17}$$

e. Outside of a cutoff radius, the first derivative with respect to energy of logarithmic derivative of each pseudo-wavefunction is identical to its corresponding all-electron wavefunction.

2) Ultrasoft pseudopotential

The goal of pseudopotential method is to make pseudo wavefunction to be "smooth" and accurate. As we discuss before, in the plane-wave calculation, the valence wavefunctions are expanded by Fourier transform into a series of plane waves. The time-consuming of this calculation are proportionally increasing with the growing number of Fourier coefficients. The smoother pseudo wavefunction means the less Fourier expansion required within an accurate calculation. Norm-conserving pseudopotential is more accurate but not smooth.

Blöchl [14] and Vanderbilt [15] proposed the concept of ultra-soft pseudopotential. According to the definition from Vanderbilt, ultrasoft pseudopotential wavefunction is no longer following the Norm-conserving pseudopotential. It is defined by Augmentation Charge (additional charge) to achieve the Generalised Norm-conserving condition. Basically, ultra-soft pseudopotential is used to fill the position left because of the electron cloud which is too localized to be eliminated. And it makes the scattering behavior around reference state energy remains scattering properties, which means rate of change is consistent.

However, according to the experiences of actual operation, coincidence degree of logarithmic derivative graph of ultra-soft pseudopotentials is not as good as of norm-conserving pseudopotentials. For instance, "generalized completely separable nonlocal pseudopotential" proposed by Blöchl, with the technology of using more than one reference eigenstates on one angular momentum, could fix the error of the scattering properties due to not comply with Norm-conserving condition. In addition, the additional charge, which is used to maintain the number of valence electrons in pseudo core, will cause the overlap operators appear in the formula for expected value. This will also cause the Kohn-Sham equation eventually becomes a generalized eigenvalue problem, rather than the general eigenvalue problem.

$$\left[-\frac{1}{2}\nabla^2+V_{\text{local}}+\delta\hat{V}_{NL}^{US}-\varepsilon_i S\right]\tilde{\psi}_i=0 \tag{1.18}$$

Ultrasoft pseudopotential not only guarantees the accuracy, but also generates a smoother pseudo-wave function which can greatly reduce the cutoff energy to reach convergence. Thus it can improve the computational efficiency and becomes the most widely used pseudopotential in *ab initio* calculations.

3) PAW method

Blöchl [16], Kresse and Joubert [17] re-clarified the orthogonal plane wave (OPW) method to adapt to the modern algorithms which is to calculate energy, power and stress, in order to develop a new kind of pseudo-potential method, called the projector augmented wave (PAW) method.

Just like ultra-soft pseudopotential, PAW method also introduces local functionals for projection and auxiliary, and expressed the wave function as a superposition of a smooth function and core function. This method can effectively be used to solve the generalized eigenvalue problem. The first advantage of projected augmented wave method is to effectively improve the shape of

potential function. PAW method could also maintain every all-electron function and greatly improve the calculation accuracy of First Principle in magnetic materials, alkali and alkaline earth metals, 3d transition elements, lanthanides and actinides and rare earth elements. As VASP provides PAW pseudopotentials of almost all elements, it's very convenient for users. The developer of VASP claims, PAW method can provide the same calculation accuracy as all-electronic methods (such as FLAPW method), while with higher computational efficiency, which makes it better for large systems.

1.3.5 The algorithm of electronic structure calculations

At present, there are three methods to solve the problem of isolated particles at electronic state, respectively as follow: 1) the plane wave and grid method; 2) linear combination of atomic orbitals (LCAO); 3) atomium method. These three methods are fundamentally the same. If used them properly and tested convergence carefully, each method can satisfy the problems on electronic structure calculations, and they can all develop into a complete set of frame for more accurate calculation. Of course, each method has its advantages and disadvantages. Usually each method is more suitable for one certain problem which can give specific information for this problem. If the user cannot understand these methods clearly, there might be some mistakes to overlook or cause unreasonable results.

1.3.6 The limitations of density functional theory

After decades of development, DFT makes a more convenient method for material design, so that it has important applications in physics, chemistry, materials, even the biological fields.

But there are still some limitations in DFT, such as 1) the famous “energy band problem”, the energy bands of semiconductors and insulators calculated by DFT are usually lower than the actual value. The possible solutions are applying more accurate hybrid functional, or LDA+U method, quasi-particle approximation (GW) method, or a self-acting correction (SIC) and so on to increase the correlated energy band gap. 2) overbinding problem: the lattice constant value of equilibrium structure obtained through the L(S)DA method is usually less than the true value, while the bulk modulus and binding energy are too high. The calculation results with the GGA method may be much better, but for some heavy elements, the values of the optimized lattice constant from GGA method are usually larger than the true values. 3) Poor description of strongly correlated systems .It usually underestimated the exchange splitting of d band and f band. Some transition metal compounds, actually Mott insulator or charge-transfer insulators, are often calculated to be be metal. The solution of this problem is the same as the first one. 4) DFT method is not accurate for vdW interaction system. Although LDA is not included in vdW interaction, due to LDA has the overestimated binding energy and there is over-binding effect, the calculated results from the methods considering vdW interaction are closer to the true value. For example, the recent studies of carbon nanotubes, nanobelts and other systems are made by DFT-LDA method. Since the error is too large, GGA method completely does not apply to these systems.

After all, one of the most important topics in DFT is how to take into account of vdW interaction in exchange-correlation effects and implemented on the algorithm.

To overcome these limitations, scientists has extended DFT, such as applying LDA+U method to study strongly correlated systems, using time-dependent density functional theory (TDDFT

[18]) to calculate the excited state properties, using GW method [4] to calculate the energy band, using Car-Parrinello method to simulate dynamic properties of system, etc.

Chapter 2

Evolutionary Algorithm of Crystal Structure Prediction: USPEX

Crystal structure prediction (CSP) is to find the most stable arrangement of atoms given only the chemical composition. The two main problems we were facing are searching for the efficient exploration of the multidimensional energy landscape and ranking the correct calculation of relative energy [19]. To search for the global minimum, we need two levels of optimization: global optimization and local optimization. In this chapter, I will introduce the evolutionary algorithm USPEX.

2.1 Background and Development

As the stable structure corresponds to the global minimum of the free energy surface, crystal structure prediction is mathematically a global optimization problem.

Recent developments provide some efficient methods to solve the searching problem, such as in 1992, the random sampling was proposed by Freeman and Catlow. Also, there are methods like simulated annealing (Deem and Newsam 1989; Pannetier et al. 1990; Boisen et al. 1994; Schön and Jansen 1996), molecular dynamics and metadynamics (Martoňák et al. 2003, 2005, 2006), data mining (Curtarolo et al. 2003) and minima hopping (Gödecker 2004). All of them rely on local optimization methods. And these methods start searching in a good region of configuration space so that efforts are not wasted on sampling poor regions. However, each of these methods may have some defects. For data mining, it is to compare the free energies of numbers of candidate structures and could indicate a list of likely ones efficiently. But it has problem when predicting a stable but totally unknown structure [20].

On the other hand, the others just locate and find the best structures by a "self-improving" method, such as evolutionary algorithms. This kind of simulations only requires the information about the chemical composition and previous studies of structure prediction have laid the foundation for them. The evolutionary algorithm USPEX (Universal Structure Predictor: Evolutionary Xtallography) has been developed to overcome the drawbacks of the preceding algorithms, and provide a new pattern with *ab initio* methods to predict crystal structures which contain up to 30-40 atoms in the unit cell.

2.2 Global Optimization

2.2.1 Complexity of the Problem and Energy landscape

Global optimization is the main problem for Crystal Structure Prediction. It is important to explore the energy landscape firstly. The number of possible distinct structures on the landscape can be evaluated as:

$$C=\binom{V/\delta^3}{N}\prod_i\binom{N}{n_i} \tag{2.1}$$

where N is the total number of atoms in the unit cell of volume V, δ is a relevant discretization parameter (for instance, 1 Å) and n_i is the number of atoms of i-th type in the unit cell. Also for small systems (N ≈ 10-20), C is astronomically large (roughly 10^N if one uses δ=1Å and typical atomic volume of 10Å^3) [19].

To understand more clearly, we can consider the dimensionality of the energy landscape as:

$$d=3N+3 \tag{2.2}$$

3N-3 degrees of freedom are the atomic positions, and the six dimensions left are defined as lattice parameters. With an increasing dimensionality, the random search will be very difficult to find the ground state, because of the inverse relationships between order and energy and between the dimensionality and diversity of crystal structures [19]. Especially for some high-dimensional problems, using this kind of search method to find a stable structure is absolutely exhaustive.

The global optimization problem can be greatly simplified if the structure is relaxed. During relaxation (local optimization), structures are brought to the nearest local energy minima and all these local minima could form as a reduce energy landscape, which is much more efficient to fine a new structure. The intrinsic dimensionality of this reduced energy landscape can be reduced as:

$$d^* = 3N + 3 - \kappa \tag{2.3}$$

where κ is the (noninteger) number of correlated dimensions. From this formula, we can see the d* depends both on system size and on intrinsic chemistry of system. We found 2d*=10.9 (d=39) for Au_8Pd_4, and the dimensionality of $Mg_{16}O_{16}$ drops dramatically from 99 to 11.6. Accordingly, the complexity for energy landscape is:

$$C^* = \exp\left(\beta d^*\right) \tag{2.4}$$

with β < R, d* < d, and C*«C, implying that local optimization could increase the efficiency of global optimization method, even for simple random sampling. All the current global optimization methods assume the landscape should have an overall "funnel" shape to be optimized. For instance in Figure 2.1a, usually the original response surface is huge and "noisy" (such as contains very large energy variations or with high barriers). The global minimum is surrounded with many very good local minima. Local optimization reduces this surface to local

minima points and the reduced surface has a simple overall shape, which is necessary to be optimized [21]. Figure 2.1b is a 2-D representation of the energy landscape of Au_8Pd_4 system using this method [22]. The surface has the same meaning as the dashed line in Figure 2.1a.

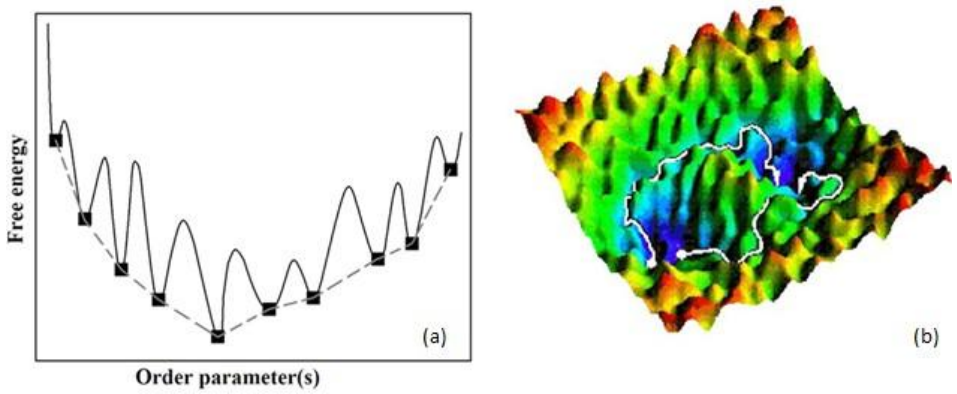

Figure 2. 1: (a) 1D scheme showing the full energy landscape (solid line) and reduced landscape (dashed line joining local minima); (b) 2D projection of the reduced energy landscape, showing clustering of low-energy structures in one region.

2.2.2 Methodology of evolutionary algorithm

The evolutionary algorithm USPEX (Universal Structure Predictor: Evolutionary Xtallography), includes local optimization and treats structural variables as physical numbers. It starts a calculation of new candidate structure from a set of parent structures, which is called population. Then the structures are evolved mainly by operators -- heredity, mutation and permutation. The fitness of structures is the relevant thermodynamic potential derived from *ab initio* determination. The powerful searching of this method is invariant with the system and a self-improved learning process.

Figure 2.2 is a conclusion diagram about how USPEX works for Crystal Structure Prediction: Firstly, the initialization of the first generation, that is, new candidate structures that tested against three constraints are randomly generated. Then, we apply a local optimization of the fittest structures by *ab initio* total energy calculation of the population. The selection of the best

structures from the current generation as parents is created by applying variation operators. And the worst structures of a population are discarded. At last, evaluate the quality for each new structure of the population and repeat the last two steps in a loop until the target structure is achieved.

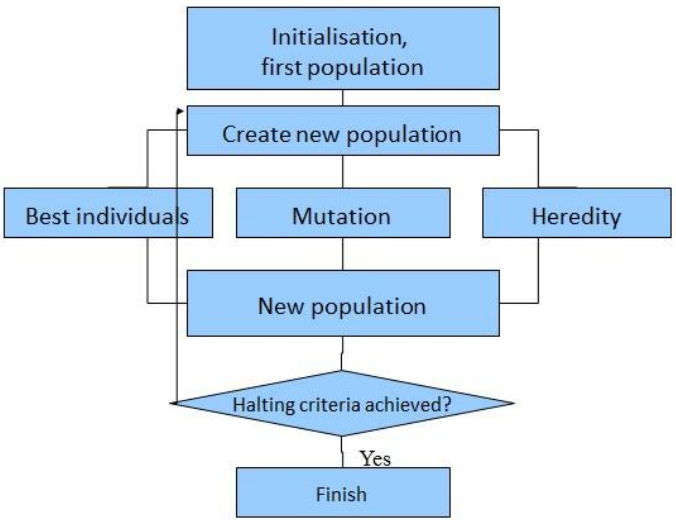

Figure 2. 2: Illustration of the evolutionary algorithm for crystal structure prediction

The above algorithm has been implemented in the USPEX code [23]. For Crystal Structure Prediction firstly, it is to search for the structure with the lowest enthalpy. And local optimization creates chemically reasonable local environments for the atoms.

2.2.3 Variation operators

The evolutionary algorithm generates offspring structures through selection of the low-energy structures to become parents of the new generation, survival of the fittest structures, and applying variation operators. This is another success of USPEX, in general, the choice of variation operators in Figure 2.3. Heredity is the core part of the evolutionary algorithm, which creates off-spring by combing coherent slabs and weighting the lattice vectors matrices averagely from two or more parents. Mutation operators use a single parent to produce one offspring structure that

has random deformation applied to the unit cell shape. Softmode mutation displaces the atoms along the softest mode eigenvectors, or a random linear combination of softest eigenvectors [24]; permutation operator swaps chemical identity in chemically different atoms. There are also some special coordinate mutations which are displacements of the atoms.

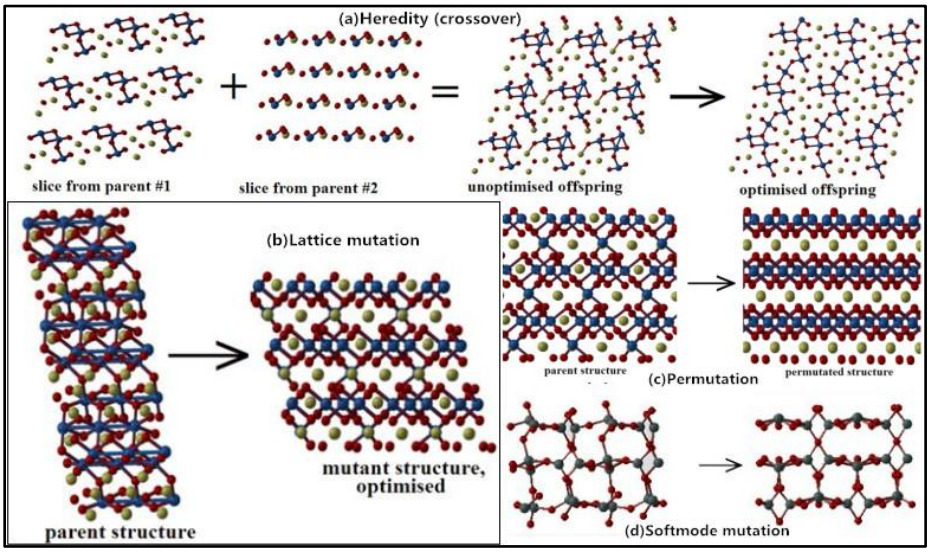

Figure 2. 3: Variation operators: a. Heredity (crossover); b. Lattice mutation; c. Permutation; d. Softmode mutation [24]

2.3 Applications of USPEX

So far, the USPEX method has been successfully applied to different kinds of systems, such as molecular crystals, variable compositions, surfaces and clusters. And the results from these applications are efficient and quite encouraging. To predict very large and complex crystal structures, this method has made many progresses.

For example, one of the successful tests is for a Lennard-Jones crystal with 128 atoms in the supercell with variable composition structure search, which has correctly identified hcp structure as the ground state within 3 generations (each consisting of only 10 structures) [20,25]. This application for variable composition system illustrated how to deal with a complex energy

landscape consisting of compositional and structural coordinates. And it is no longer just one dimensional to optimize, but a two dimensional convex hull representation (as in Figure 2.4).

Another illustration of how USPEX works is also the largest test and the longest run for a chemically complex system. It's the prediction of the correct ground-state structure of post-perovskite using a relatively large 80-atom supercell and an empirical potential describing interatomic interaction within a partially ionic model [26]. With 80 atoms per cell, the post-perovskite structure was relaxed during about 3200 local optimizations. This is the typical example of USPEX for a fixed composition system.

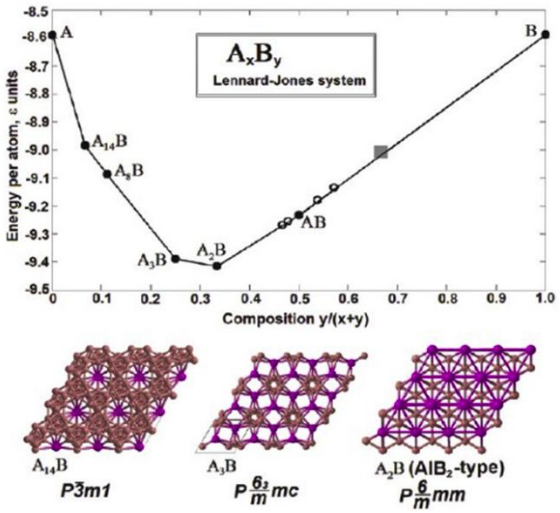

Figure 2. 4: Using USPEX simulation for the variable-composition of the AxBy binary Lennard-Jones system. Solid circles represent for stable compositions, open circles denote marginally unstable compositions (A_8B_7, $A_{12}B_{11}$, A_6B_7 and A_3B_4). Gray square fixed-composition results for AB_2 stoichiometry. The lower panel shows some of the stable structures [25].

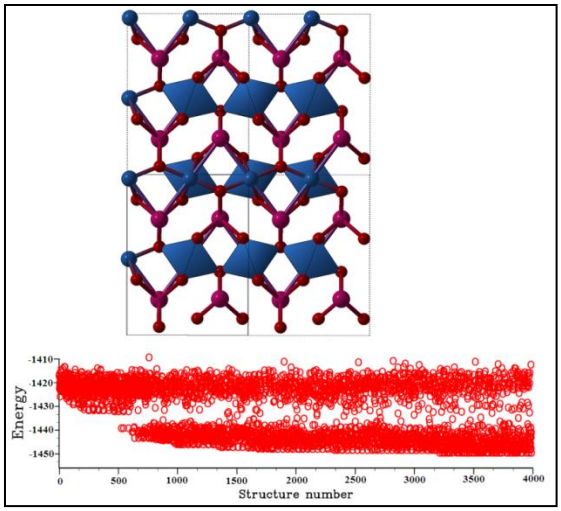

Figure 2. 5: An example of a test on the prediction of the crystal structure of $MgSiO_3$ with 80 atoms in the super cell. The lower panel shows that the global-minimum structure was found with 3200 structural relaxations. Taken from Ref [26].

Chapter 3

The Prediction of Stable Compounds in the Al-O System

3.1 Introduction and background

In the crust, oxygen and aluminum have the first and third highest abundance among all elements, respectively. Also aluminum is the most abundant metal element, which constitutes up to 7.57% by mass. Until now, there are more than 1000 mineral species known to contain aluminum. Aluminum is a good conductor of electricity and heat, while alumina is an insulator. But alumina is suitable for abrasive materials and cutting tools. Activated alumina could also be used as catalyst, adsorbent, dehydrating agent and a catalyst carrier. Alumina is an important ceramic material and a major chemical component of the Earth. The knowledge of other thermodynamically stable compounds in the aluminum oxide system is consequently important to better understand physics and chemistry of the Earth and planetary interiors. Accordingly, aluminum oxides interest scientists in earth and material sciences for theoretical and experimental studies.

The most common aluminum oxide is alumina, which is an important ceramic material and a major chemical component of the Earth. Under high pressure, alumina is used as an optical window material in shock-wave experiments and is incorporated into mantle minerals and significantly affects their physical properties [27,28]. Concluded from previous studies, there are several phase transitions have been theoretical predict and experimental confirmed. $R\bar{3}c$ corundum phase transforms to the Pbcn Rh_2O_3(II) structure at about 100 GPa and high temperature [29,30]. And above 130 GPa, the Pbcn Rh_2O_3(II)-type alumina adopts the Cmcm $CaIrO_3$-type Al_2O_3 (post-perovskite structure) [31,32]. In 2007, Umemoto K and Wentzcovitch

KM predict a phase transition in alumina at about 370 GPa and room temperature, from the $CalrO_3$-type polymorph to another with the U_2S_3-type structure [33].

Among various Al_xO_y species, the simplest polyatomic representatives are Al_2O and AlO_2. In experimental studies, scientists already have discovered evidences for AlO_2. For instance, peroxide oxide was shown to form by an interfacial reaction in the presence of a kinetic constraint during diffusion-bonding of Pt and α-Al_2O_3. Raman spectroscopy on AlO_2 has provided strong evidence for its presence [34]. It formed after heating for 24 hours in the temperature range of 1200 to 1400℃, but not at or below 1100℃.

During previous work, for instance, in the Na-Cl system under high pressure, Oganov et al. have already predicted some novel stable compounds of unusual stoichiometries (Na_3Cl, Na_3Cl_2, $NaCl_3$ and $NaCl_7$) which have been confirmed by the experiments [35]. If this unusual situation could also exist in the Al-O system, this will have significant implications in physics and material sciences. And we have explored this possibility and found two thermodynamically stable compounds in this system with very interesting crystal structures and unusual chemical bonds. These compounds also exhibit some distinct properties that I will introduce in Section 3.4.

3.2 Methods

To predict new stable structures in the fixed chemical composition Al-O system, we used the evolutionary algorithm USPEX to search for the structure with the lowest enthalpy at pressures range from 0 to 500 GPa and temperature at 0 K. During the initialization, USPEX operates with populations of structures and select the parent structures from them. Then offspring structures are generated through variation operators by *ab initio* total energy calculation of the population. Stable compositions are determined using the convex hull construction, also called local

optimization: verify a compound is thermodynamically stable according to its enthalpy of forming by any other compounds is negative. Our prediction was using *ab initio* structure relaxations based on density functional theory (DFT) within the Perdew-Burke-Ernzerhof (PBE) generalized gradient approximation (GGA) [36], as implemented in the VASP code [37].For structural relaxation, all-electron projector-augmented wave (PAW) method [38] and plane wave basis set are used in our calculation. All structures were relaxed at constant pressure and 0 K. The energetically worst structures were discarded and a new generation was created by 20% randomly from space group, 40% produced by heredity and 40% from the remaining structures through softmutation and transmutation of atoms. Such calculations provide an excellent description of the new structures (AlO_2, Al_4O_7) and their energetics. Then we calculated phonon frequencies throughout the Brillouin zone using the finite displacement approach as implemented in the Phonopy code [39]. And together with the computed results from energy of band structure and density of states of these two new compounds, we can make sure that the obtained structures are dynamically stable.

3.3 Thermodynamically stable aluminum oxides Al_4O_7 and AlO_2

For the Al-O system, we searches for stable structures in the unit cell with maximum 20 atoms at pressures in the range of 0-500 GPa. These searches yielded α-Al_2O_3 as a stable oxide under all pressures, but more surprisingly, there are two new compounds predicted to be stable under higher pressures. To confirm and to obtain the most accurate results, we then focused on structure optimization for these new compounds. We found two of them, AlO_2 and Al_4O_7, are thermodynamically stable and performed further study about their different properties.

3.3.1 Phase diagram of the Al_2O_3-O system

As in the Al_2O_3-O phase diagram, there are several results from the USPEX calculation. First of all, Al_2O_3 is predicted to undergo a phase transition induced by pressures from Cmcm to Pnma. Cmcm $CaIrO_3$-type Alumina is stable until Al_2O_3 eventually adopts the Pnma structure above 394 GPa. In Figure 3.2, we compare the Pnma-Al_2O_3 with U_2S_3-type Al_2O_3 structures, which also is a Pnma structure under high pressure from the Ref [40], and calculate their formation enthalpy. Accordingly, we found the same stable structure as U_2S_3-type Al_2O_3.

In addition, Al_4O_7 begins to show competitive enthalpy of formation at pressures above 300 GPa. Until the pressure increases to 500 GPa, we find AlO_2 becomes thermodynamically stable. And this new compound AlO_2 has a monoclinic structure with the space group $P2_1/c$. For more accurate results, using local optimization to compare the formation enthalpies of each compounds, we found C2-Al_4O_7 is stable from 330 to 443 GPa. And AlO_2 starts to become stable near 322 GPa with space group $P2_1/c$. For AlO_2, at 500 GPa, the enthalpy of formation becomes impressively negative, -0.115 eV/atom, from Al_2O_3 and O_2.

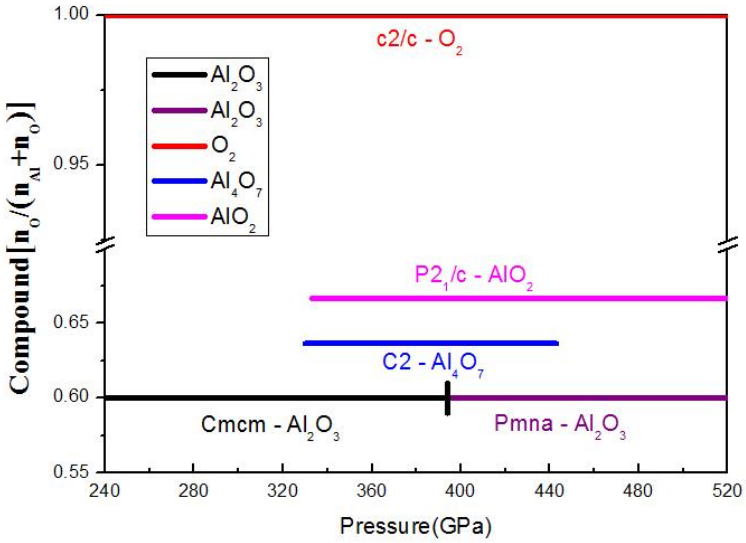

Figure 3. 1: Phase diagram of Al_2O_3 -O system. Al_2O_3 has a phase transition from Cmcm-space group at 394 GPa. From 330 to 443 GPa, C2-Al_4O_7 becomes stable. And AlO_2 starts to become stable with $P2_1/c$ space group upon 322 GPa.

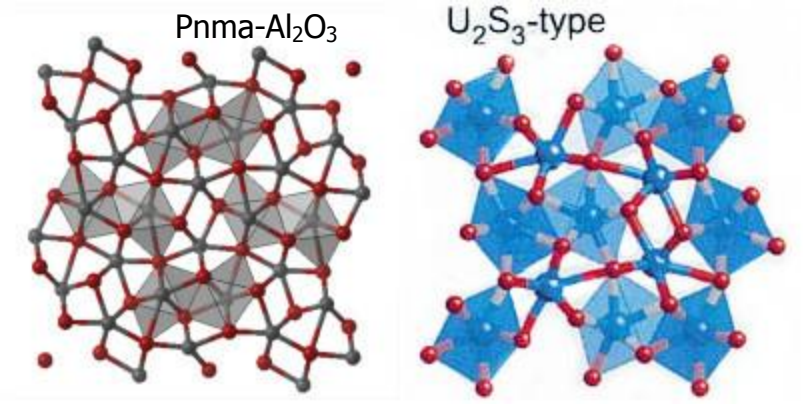

Figure 3. 2： Crystal structures of Pmna-Al_2O_3 (left) and U_2S_3 type-Al_2O_3 (right). Grey (Blue in figure b) and red spheres denote aluminum and oxygen, respectively.

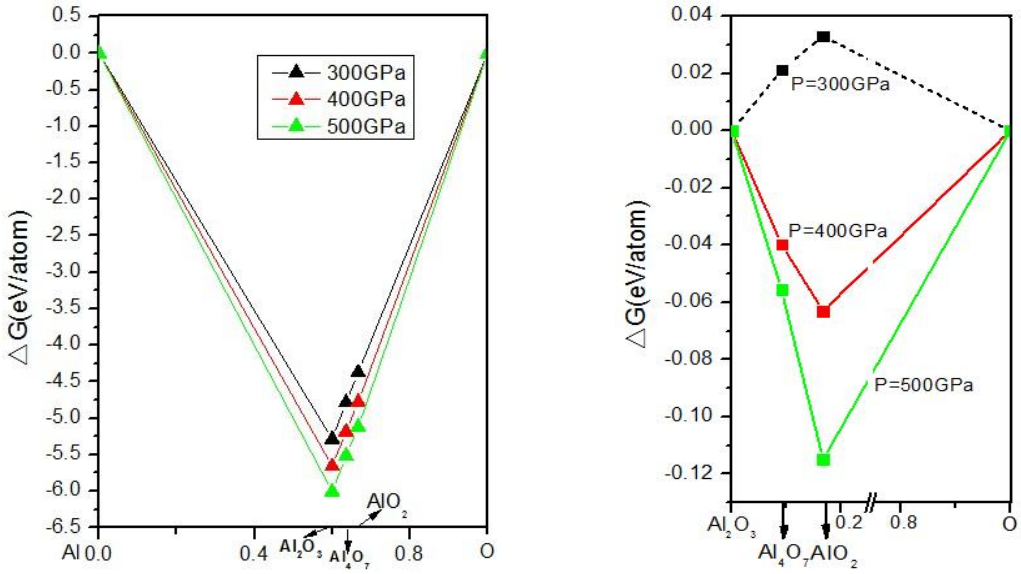

Figure 3. 3: Convex hull for the Al-O and Al_2O_3-O system at high pressures; for oxygen, we used the previous structure predicted from Ref [41]. From the Al_2O_3-O convex hull, AlO_2 is stable at both 400 and 500 GPa and Al_4O_7 is stable at 400 GPa, which correspond to the results from the phase diagram.

3.3.2 Structures of stable compounds: Al_4O_7 and AlO_2

These two compounds both contain O^{2-} and $[O\text{-}O]^{2-}$ anions. The peroxide ion is composed of two oxygen atoms that are linked by a single bond. In Figure 3.4a, there are one $[O\text{-}O]^{2-}$ anion in the Al_4O_7 with C2 structure and the bonding length is 1.43Å. And as shown in Figure 3.4b, this structure of Al_4O_7 can be seen as a packing of O atoms and aluminum ion layers. According to

the bonding situation, the chemical formula can also be written as $[Al_4O_5(O\text{-}O)]$ for better understanding the chemical composition.

Also, above 322 GPa, there is AlO_2 with space group $P2_1/c$ and 6 Al-O coordination number, which is stable as $[Al_4O_4(O\text{-}O)_2]$. As seen from the formula and Figure 3.5, AlO_2 has three peroxide ions and three oxide ions per lattice. The $[O\text{-}O]^{2-}$ bond length is 1.38Å. Each Al^{3+} is coordinated with three $[O\text{-}O]^{2-}$ anions. The O-O bond distance in oxide O^{2-} is 1.33 Å and is 1.21 Å in O_2 molecule. And 0 GPa, the bond length is 1.49 Å in O_2^{2-}.

All the lattice constants and atomic positions of these two structures are concluded in Table 3.1 and 3.2.

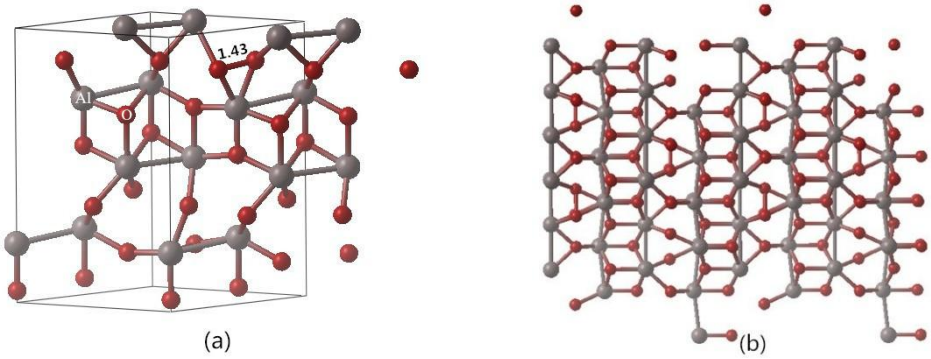

Figure 3. 4: Structure of Al_4O_7. (a) The $[O\text{-}O]^{2-}$ bond length is 1.43Å; (b) the aluminum atoms are forming layers and coordinated with oxide and peroxide ions.

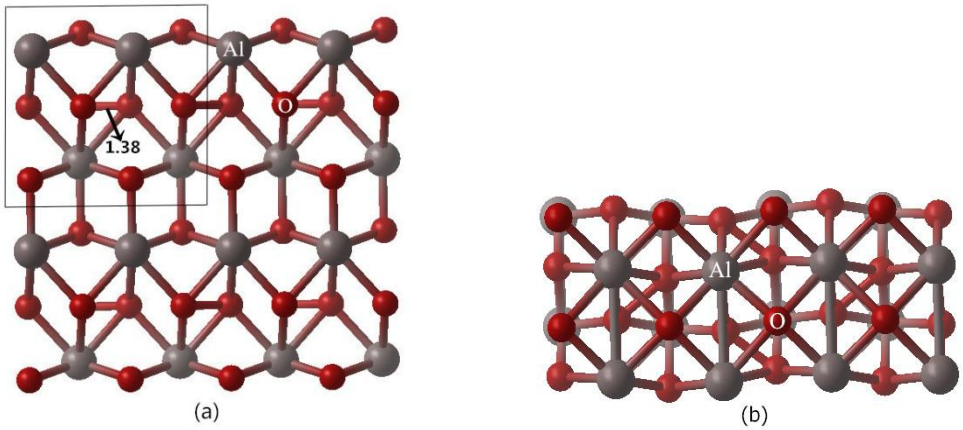

Figure 3. 5: Structure of AlO_2. (a) The bond length of peroxide ion is 1.38 Å; (b) Each Al atom is coordinated with three $[O\text{-}O]^{2-}$ anions.

Elements	Structures	Lattice Constants (Å)	Atomic Positions
Al	C2	α=4.59820 β=9.66989 γ=5.09398	4c (0.270023,0.000090,0.521555)
			2a (0.000000,0.258021,0.000000)
			2a (0.500000,0.285882,0.000000)
O	C2		2a (0.000000,0.439930,0.000000)
			4c (0.262381,0.129869,0.911020)
			4c (0.253380,0.313967,0.504568)
			2b (0.500000,0.132414,0.500000)
			2a (0.500000,0.456751,0.000000)

Table 3. 1: Lattice constants and atomic positions of Al_4O_7 with C2 structure.

Elements	Structures	Lattice Constants (Å)	Atomic Positions
Al	$P2_1/c$	α=4.66484 β=2.30360 γ=4.72564	2a (0.221669,0.275015,0.631539)
O	$P2_1/c$		2a (0.133908,0.758225,0.876831)
			2a (0.501572,0.183121,0.384900)

Table 3. 2: Lattice constants and atomic positions of AlO_2 with $P2_1/c$ structure.

3.4 Some material properties of the two new compounds

The band structure for these compounds was calculated, to produce accurate band gaps for comparing their electronic properties. Al_4O_7 has a narrow band gap with 2.57 eV energy at 400 GPa, which is an insulator. AlO_2 is also an insulator with band gap energy (3.01 eV) at 400 GPa, as in Figure 3.6. Also, unlike the band structure of Al_2O_3, both Al_4O_7 and AlO_2 have the low conduction band between high conduction band and valence band. According to the electron structure calculation, we can get these low conduction bands are generated because of the peroxide ions, as in Figure 3.6c. This conclusion can also get from calculation results of the density of states as below.

Phonon calculations in Figure 3.7 for Al_4O_7 and AlO_2 at 400 GPa show that no imaginary phonon frequencies exist throughout the Brillouin zone, suggesting that these structures are dynamically stable. For the Al_4O_7 C2 phase, there is very tiny imaginary frequency near Γ point. To find the "real" ground state, we can use powerful metadynamic method in USPEX for the structure searching.

In Figure 3.8a, O1 is the oxygen atom from peroxide bond and O2 is the normal oxygen atom from oxide ion. There is not any density of states for Al under Fermi Energy and non-negligible d-contribution, so all valence electrons are on O atoms rather than on Al. This is evidence of significantly ionic bonding which is the transfer of electrons from Al to O.

Accordingly, oxide ions and peroxide bonds are played different roles to form energy band. For AlO_2, under -20 ev, there are two peaks of O1_s orbital, which form σ and σ* orbitals. And O1_p and O2_p orbitals occupy the range from -20 to 0 ev, which suggests that HOMO (highest occupied molecular orbital) is on the peroxide bond. The LOMO (lowest occupied molecular orbital) is around peroxide bonds, which corresponds to the σ* orbital, because of the O1_p

occupied the range among 2.81 to 5.08 eV. As a result, we can get the conclusion that peroxide ions cause the generation of low conduction band that is shown in band structure (Figure 3.6a). In addition, Al_4O_7 has two peroxides bonds, O2 and O3, and five types of oxygen atoms but very similar results of density of states as AlO_2.

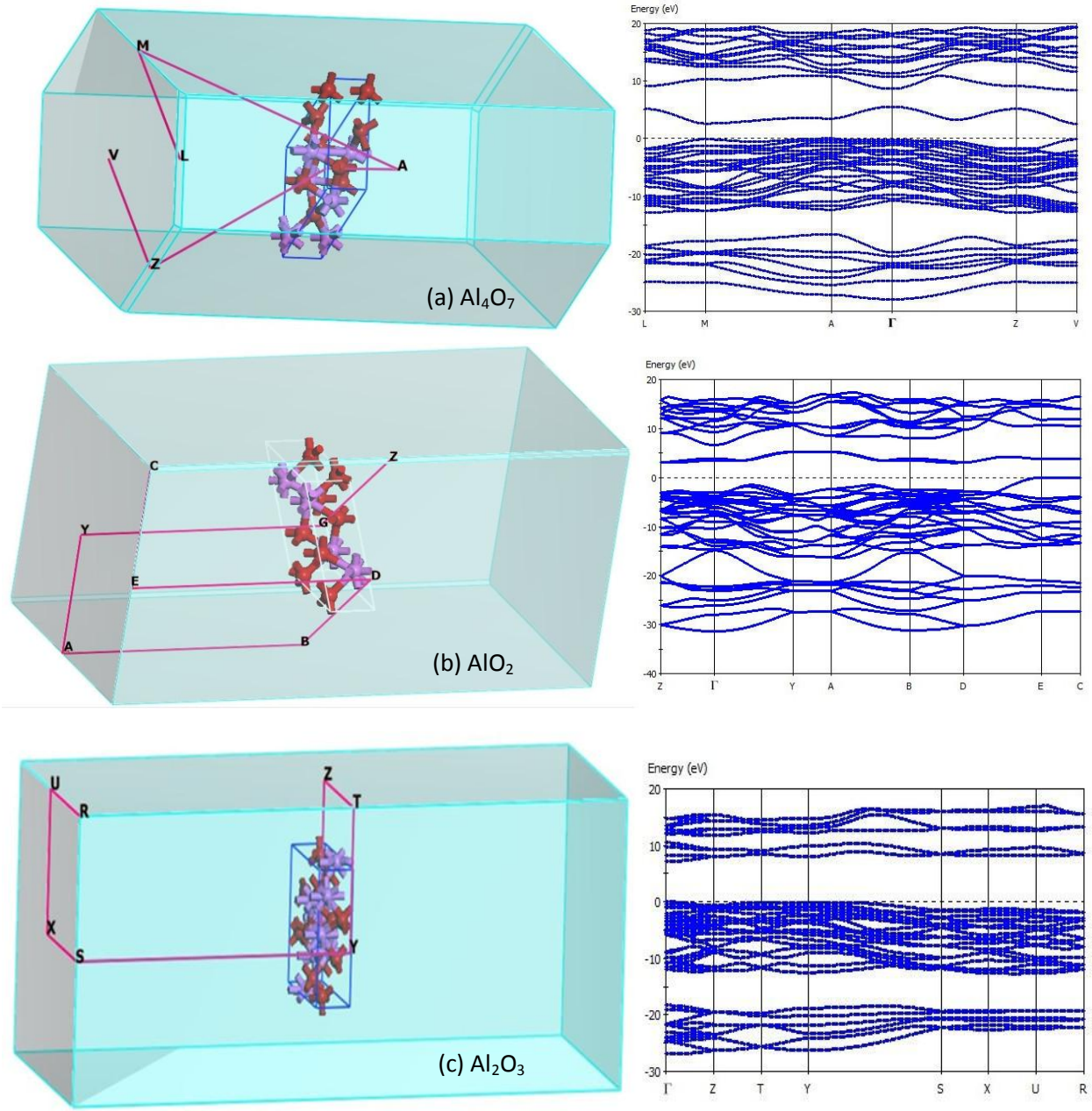

Figure 3. 6: Band structure of AlO_2 (a), Al_4O_7 (b) and Al_2O_3 (c) at 400 GPa.

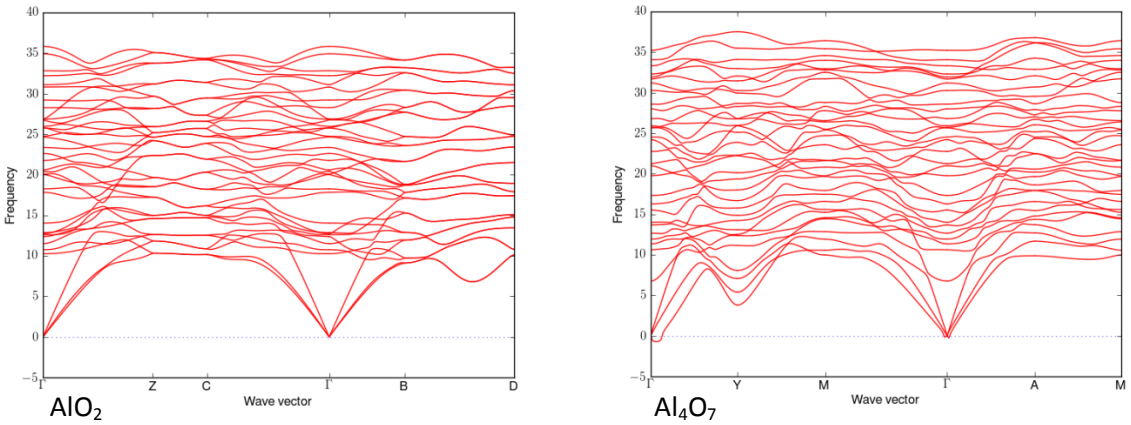

Figure 3. 7: Phonon calculation for AlO_2 (left) and Al_4O_7 (right) at 400 GPa.

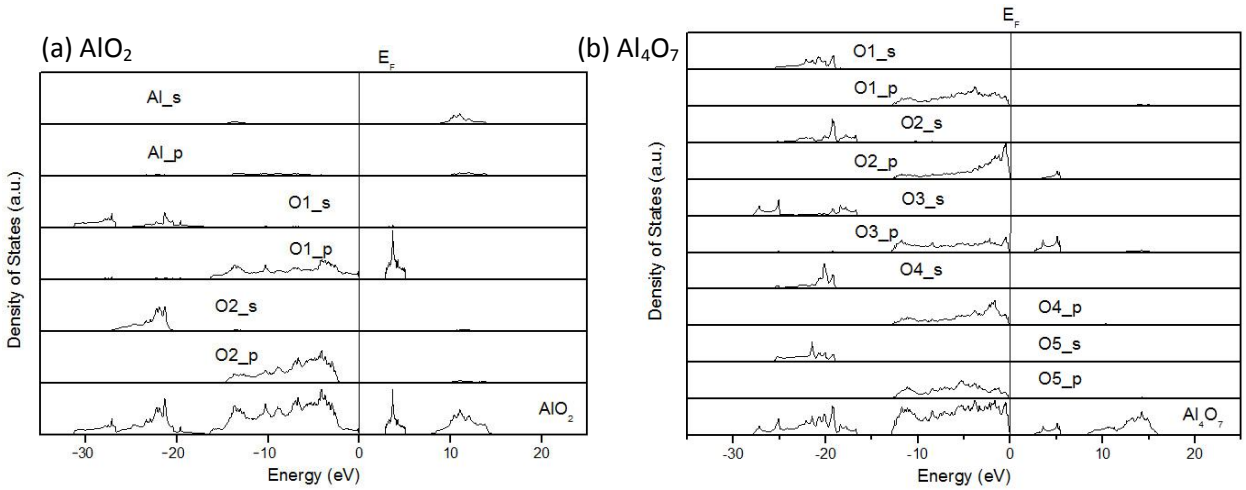

Figure 3. 8: (a) Density of states for AlO_2: O1 is atom from peroxide ions and O2 is atom from oxide ions; (b) Density of states for Al_4O_7: O1 and O2 are atoms from two respective peroxide ions, and O3, O4, O5 are atoms from three oxide ions.

4. Conclusions

In summary, according to the systematic search for the stable compounds in the Al-O system at pressures up to 500 GPa, we found that two more compounds (AlO_2 and Al_4O_7) become thermodynamically and dynamically stable above 322 GPa and in the range from 330 to 443 GPa, respectively. Our analysis reveals that in these two insulating compounds AlO_2 and Al_4O_7 exhibit significant ionic character. Both of them are stabilized by the formation of the peroxide $[O\text{-}O]^{2-}$ anion and contain by both peroxide and oxide ions. For better understanding properties about these two new aluminum compounds, we calculate density of states in this system to describe the number of states per interval of energy at each energy level that are available to be occupied by electrons. As we expected, most valence electrons are on O atoms and rather than on Al. And oxide and peroxide ions have different effects on forming conduction band.

Bibliography:

[1] R. M. Martin, Electronic structure: basic theory and practical methods, Cambridge University Press, Cambridge, 2004.
[2] D. Raabe, Computational materials Science, 2002.
[3] Reports from J. J. Zhao.
[4] N. W. Ashcroft, Electron-ion pseudopotentials in metals, Phys. Lett. 23, 48, 1966.
[5] G. X. Xu, et al., Quantum chemistry - Fundamentals and *ab initio* calculations, Beijing, China Science Press,1995.
[6] P. Hohenberg and W. Kohn, Inhomogeneous electron gas, Phys. Rev. 136, B864, 1964.
[7] W. Kohn and L. J. Sham, Self-consistent equations including exchange and correlation effects, Phys. Rev. 140, A1133, 1965.
[8] J. P. Perdew and A. Zunger, Self-interaction correction to density-functional approximations for many-electron systems, Phys. Rev. B 23, 5084, 1981.
[9] J. P. Perdew, Y. Wang, Pair-distribution function and its coupling-constant average for the spin-polarized electron gas, Phys. Rev. B 45, 13244, 1992.
[10] J. P. Perdew, K. Burke, and M. Ernzerhof, Generalized gradient approximation made simple, Phys. Rev. Lett. 77, 3865, 1996.
[11] N. W. Ashcroft, Electron-ion pseudopotentials in metals, Phys. Lett. 23, 48, 1966.
[12] A. O. E. Animalu et al., The screened model potential for 25 elements, Phil. Mag. 12, 1249, 1965.
[13] D. R. Hamann, M. Schluter, and C. Chiang, Norm-conserving pseudopotentials, Phys. Rev. Lett. 43, 1494, 1979.
[14] P. E. Blöchl, Generalized separable potentials for electronic-structure calculations, Phys. Rev. B 41, 5414, 1990.
[15] D. Vanderbilt, Soft self-consistent pseudopotentials in a generalized eigenvalue formalism, Phys. Rev. B 41, 7892, 1990.
[16] P. E. Blöchl, Projector augmented-wave method, Phys. Rev. B 50, 17953, 1994.
[17] G. Kresse, D. Joubert, From ultrasoft pseudopotentials to the projector augmented-wave method, Phys. Rev. B 59, 1758, 1999.
[18] G. Onida, L. Reining, and A. Rubio, Electronic excitations: density-functional versus many-body Green's-function approaches, Rev. Mod. Phys. 74, 601, 2002.
[19] A. R. Oganov, A. O. Lyakhov, M. Valle, How evolutionary crystal structure prediction works - and why. Acc. Chem. Res. 44, 227-237, 2011.
[20] A. R., Oganov, Y. Ma, A. O. Lyakhov, M. Valle, C. Gatti, Evolutionary crystal structure prediction as a method for the discovery of minerals and materials. Rev. Mineral. Geochem. 71, 271–298, 2010.
[21] A. R. Oganov and C. G. Glass. Crystal structure prediction using evolutionary algorithms: principles and applications. J. Chem. Phys., 124: 244704, 2006.
[22] A. R. Oganov and M. Valle, How to quantify energy landscapes of solids, J. Chem. Phys. 130, 104504, 2009.
[23] A. R. Oganov and C. W. Glass. Evolutionary crystal structure prediction as a tool in materials design. J. Phys.: Cond. Matter, 20:064210, 2008.
[24] A. L. Lyakhov, A. R. Oganov, and M. Valle. How to predict very large and complex crystal structures. J. Comput. Phys. Comm., 181:1623-1632, 2010.
[25] P. Prachi. Materials genome initiative and energy. MRS Bulletin, 36: 964–966, 2011.

[26] A. R. Oganov, S Ono, Theoretical and experimental evidence for a post-perovskite phase of MgSiO3 in Earth's D ″laye, Nature 430, 445-448, 2004.
[27] B.J. Wood & D.C. Rubie, The effect of alumina on phase transformations at the 660-kilometer discontinuity from Fe-Mg partitioning experiments. Science 273: 1522–1524, 1996.
[28] J.Z. Zhang & D.J. Weidner. Thermal equation of state of aluminum-enriched silicate perovskite. Science 284: 782–784, 1999.
[29] J.F. Lin JF, O. Degtyareva O, C.T. Prewitt, P. Dera, N. Sata, E. Gregoryanz, H. Mao, R.J. Hemley. Crystal structure of a high-pressure/high-temperature phase of alumina by in situ X-ray diffraction. Nat. Mater. 3: 390-393, 2004.
[30] R. Caracas, R.E. Cohen. Prediction of a new phase transition in Al2O3 at high pressures. Geophys. Res. Lett. 32: L06303, 2005.
[31] A. R. Oganov, S. Ono. The high-pressure phase of alumina and implications for Earth's D" layer. Proc. Nati. Acad. Sci. USA 102:10828-10831, 2005.
[32] S. Ono, A.R. Oganov, T. Koyama, H. Shimizu. Stability and compressibility of the high-pressure phases of Al_2O_3 200 GPa: Implications for the electrical conductivity of the base of the lower mantle. Earth Planet Sci. Lett. 246:326-335, 2006.
[33] K. Umemoto & R.M. Wentzcovitch. Prediction of an U_2S_3-type polymorph of Al_2O_3 at 3.7 Mbar, Proc. Nati. Acad. Sci. USA 105, No. 18: 6526-6530, 2008.
[34] Y. C. Lu, S. Agnew et al., Further characterization of the aluminum peroxide oxide, AlO_2, formed by interfacial reaction between Pt and α-Al_2O_3, Acta. Metal., mater: 43, No.5, pp. 1885-1893, 1995.
[35] W. Zhang, A. R. Oganov, A. F. Goncharov, Q. Zhu, S. E. Boulfelfel, A. O. Lyakhov, E. Stavrou, M. Somayazulu, V. B. Prakapenka, Z. Konôpková, Unexpected stable stoichiometries of sodium chlorides: Science 1459-1460, 2013.
[36] J. P. Perdew, K. Burke, and Ernzerhof M. Generalized gradient approximation made simple. Phys. Rev. Lett. 77:3865-3868, 1996.
[37] G. Kresse and J. Furthmüller. Efficient iterative schemes for *ab initio* total-energy calculations using a plane-wave basis set. Phys. Rev. B, 54: 11169-11186, 1996.
[38] P. E. Blöchl. Projector augmented-wave method. Phys. Rev. B, 50: 17953-17979, 1994.
[39] A. Togo, F. Oba, and I. Tanaka. First-principles calculations of the ferroelastic transition between rutile-type and $CaCl_2$ -type SiO_2 at high pressures. Phys. Rev. B, 78:134106, 1994.
[40] K. Umemoto K & R.M. Wentzcovitch. Prediction of an U_2S_3-type polymorph of Al_2O_3 at 3.7 Mbar, Proc. Nati. Acad. Sci. USA 105, No. 18: 6526-6530, 2008.
[41] Y. M. Ma, A. R. Oganov, C. W.Glass. Structure of the metallic ζ-phase of oxygen and isosymmetric nature of the ε-ζ phase transition: *Ab initio* simulations. Phys. Rev. B, 76: 064101, 2007.